

5-20-2013

# Formation of Cn Molecules in Oxygen-Rich Interiors of Type II Supernovae

Tianhong Yu  
*Clemson University*

Bradley S. Meyer  
*Clemson University*

Donald D. Clayton  
*Clemson University*, claydonald@gmail.com

Follow this and additional works at: [https://tigerprints.clemson.edu/physastro\\_pubs](https://tigerprints.clemson.edu/physastro_pubs)

---

## Recommended Citation

Please use publisher's recommended citation.

This Article is brought to you for free and open access by the Physics and Astronomy at TigerPrints. It has been accepted for inclusion in Publications by an authorized administrator of TigerPrints. For more information, please contact [kokeefe@clemson.edu](mailto:kokeefe@clemson.edu).

## FORMATION OF $C_n$ MOLECULES IN OXYGEN-RICH INTERIORS OF TYPE II SUPERNOVAE

TIANHONG YU, BRADLEY S. MEYER, AND DONALD D. CLAYTON  
Department of Physics and Astronomy, Clemson University, Clemson, SC 29634-0978, USA  
*Received 2013 January 22; accepted 2013 April 2; published 2013 May 2*

### ABSTRACT

Two reaction-rate-based kinetic models for condensation of carbon dust via the growth of precursor linear carbon chains are currently under debate: the first involves the formation of  $C_2$  molecules via radiative association of free C atoms, and the second forms  $C_2$  molecules by the endoergic reaction  $CO + C \rightarrow C_2 + O$ . Both are followed by C captures until the linear chain eventually makes an isomeric transition to ringed carbon on which rapid growth of graphite may occur. These two approaches give vastly different results. Because of the high importance of condensable carbon for current problems in astronomy, we study these competing claims with an intentionally limited reaction rate network which clearly shows that initiation by  $C + C \rightarrow C_2 + \gamma$  is the dominant pathway to carbon rings. We propose an explanation for why the second pathway is not nearly as effective as its proponents calculated it to be.

*Key words:* atomic processes – ISM: abundances – ISM: general – meteorites, meteors, meteoroids – supernovae: general – supernovae: individual (SN 1987A)

### 1. INTRODUCTION

Whether carbon dust can or cannot condense in the interiors of expanding Type II supernovae (SNeII) is an important question for astronomy. Many have assumed, guided by chemical equilibrium, that carbon condensation cannot occur unless carbon is more abundant than oxygen. This assumption limits C condensation to the He-burning shell of SNII. This rule of thumb was challenged when Clayton et al. (1999) introduced a non-equilibrium kinetic theory by which carbon can condense thermally in gas having more abundant oxygen, opening the possibility of C condensation throughout the O-rich core. This initial theory has been amplified by several studies (Clayton et al. 2001; Deneault et al. 2003, 2006; Clayton 2011, 2013). Within their chemical model, Cherchneff & Dwek (2009, 2010) raised questions about the most effective way of producing  $C_2$  molecules, which is the first step to linear carbon chains. They discovered that the neutral-neutral reaction  $CO + C \rightarrow C_2 + O$  has a reasonably large cross section ( $\sigma v$ ) =  $k_{CO,C} = 8.6 \times 10^{-14} \text{ cm}^3 \text{ s}^{-1}$  at temperatures near 5000 K despite being endothermic by 4.8 eV. Although the CO target abundance for the production of  $C_2$  must be calculated in this manner, they stated that in their model at  $T = 5000 \text{ K}$  it created  $C_2$  much more rapidly than the slow radiative reaction  $C + C \rightarrow C_2 + \gamma$ . Sensing high importance of this reaction for astronomy, they claimed in their list of conclusions: “A new pathway to the formation of carbon chains is active in the O-rich mass zone of the unmixed ejecta and is identified as the CO conversion to  $C_2$  via collisions with C” (Cherchneff & Dwek 2009, p. 660). Cherchneff & Dwek (2009) were unable to evaluate the quantitative consequences because their reaction network terminated at  $C_3$  and did not include the formation of linear carbon chains  $C_n$  and their isomerization to carbon rings. Cherchneff & Dwek (2010) subsequently did include linear chains to  $n = 10$ , which they took to isomerize instantly to a ringed structure, following the published model by Clayton et al. (1999, 2001).

Testing their calculated abundances for  $C_n$  is but a secondary goal of the present study. Its overriding goal is to point out abundance differences of several orders of magnitude for the CO and  $C_2$  molecules between the computations of these two

groups and to resolve those differences if possible. This test has important consequences for the condensation of carbon dust, changing prior expectations of the production of  $C_2$  owing to the reaction  $C + C \rightarrow C_2 + \gamma$  severely underestimates the subsequent abundances of linear carbon chains. Cherchneff & Dwek (2009, 2010) harbored that expectation of underestimated  $C_2$  owing to their belief that much more  $C_2$  is made earlier near  $T = 5000 \text{ K}$  and survives the high temperature. The dust created by SN expansions is currently under intense study owing to three types of astronomical observations: (1) dust observed in single SN remnants, (2) dust observed in early low-metallicity galaxies, and (3) SN-condensed carbon dust (SUNOCONs) extracted from meteorites. Each of these topics depends sensitively on how much carbon, both numbers and sizes, is able to condense in cooling SNII interiors. Therefore, we study this competition carefully.

Crucial to this task is the lifetime  $\tau_{CO}$  of CO molecules. Thermal dissociation of CO is dominated by thermal photons because radiative association of C and O dominates other reactions for the formation of CO at the densities within SNII. Each reaction and its inverse is subject to the quantum principle of detailed balance. The thermal photodissociation lifetime  $\tau_\gamma$  is calculated from the detailed balance with the radiative association reaction, as in Section 2.1 of Clayton et al. (2001). Because of the large 11.1 eV binding energy of the CO molecule,  $\tau_\gamma$  is very temperature-sensitive. For readers’ numerical ease, we will tabulate  $\tau_\gamma$  at selected key temperatures in Table 1. The flux and spectrum of newly injected Compton electrons (Clayton & The 1991) yields the lifetime  $\tau_e$  of CO molecules against inelastic scattering dissociation by Compton electrons caused by  $^{56}\text{Co}$  radioactivity. In a gas of pure CO, the mean energy per ion pair is defined as the energy of primary electrons divided by the number of pairs produced. Liu & Victor (1994) calculated the mean energy per ion pair in pure CO gas and obtained the result  $\Delta E = 32.3 \text{ eV}$  deposited per dissociated CO pair, agreeing with the measurement of 32.2 eV by Klots (1968). Thus the efficiency of energetic electrons for dissociating CO seems well established. A lifetime  $\tau_{CO}$  near one week is typical in SN 1987A, but would be longer in SNII synthesizing less  $^{56}\text{Co}$  and at times greater than about eight months.

**Table 1**  
Values of  $\tau_\gamma(\text{CO})$  and Related Quantities at Selected Time  $t$  and Temperature  $T$

$t$ (s)	$(t/t_{6000\text{ K}})^{-3}$	$T$ (K)	$\tau_\gamma$ (s)	$k_{\text{CO}}$ ( $\text{cm}^{-3}\text{ s}^{-1}$ )	$n_{\text{CO}}^{\gamma\text{eq}}$ ( $\text{cm}^{-3}$ )
$5.47 \times 10^6$	1	6000	$4.22 \times 10^{-2}$	$3.13 \times 10^{-17}$	$1.32 \times 10^1$
$5.97 \times 10^6$	0.769	5500	$3.54 \times 10^{-1}$	$2.99 \times 10^{-17}$	$6.27 \times 10^1$
$6.57 \times 10^6$	0.578	5000	$4.46 \times 10^0$	$2.83 \times 10^{-17}$	$4.24 \times 10^2$
$7.30 \times 10^6$	0.422	4500	$9.70 \times 10^1$	$2.67 \times 10^{-17}$	$4.61 \times 10^3$
$8.21 \times 10^6$	0.296	4000	$4.43 \times 10^3$	$2.48 \times 10^{-17}$	$9.67 \times 10^4$
$9.38 \times 10^6$	0.198	3500	$5.86 \times 10^5$	$2.28 \times 10^{-17}$	$5.26 \times 10^6$
$1.09 \times 10^7$	0.125	3000	$3.77 \times 10^8$	$2.05 \times 10^{-17}$	$1.21 \times 10^9$

## 2. THE PHYSICAL MODEL AND NETWORK

Because our goal is to study the chemistry, we can take a very simple physical model of the expansion, namely, temperature  $T = 3800\text{ K}/(t/100\text{ days}) = 3.30 \times 10^{10}/t(\text{s})\text{ K}$ , where  $t$  is the time elapsed since core collapse. We choose  $n_{\text{O}} = 10^{10}\text{ cm}^{-3}$  and  $n_{\text{C}} = 10^9\text{ cm}^{-3}$  at the starting time  $t = t_{6000\text{ K}}$  at  $T = 6000\text{ K}$  for our chemical network. From our model choice for  $T(t)$  we get  $t_{6000\text{ K}} = 5.47 \times 10^6\text{ s}$ . At subsequent times,  $n_{\text{O}}(t) = 10^{10}\text{ cm}^{-3}(t/t_{6000\text{ K}})^{-3}$  owing to homologous expansion. Let  $N$  be the number of any specific molecular species in a comoving, expanding, and initially  $1\text{ cm}^3$  volume at  $6000\text{ K}$ . The only change of  $N$  during expansion occurs through chemical reactions.  $N$  may be expressed as atom fraction  $Y$  of the initial total number  $N_{\text{O}} + N_{\text{C}} = 1.10 \times 10^{10}$  atoms. We intentionally choose an O-rich interior having  $N_{\text{O}}/N_{\text{C}} = 10$ , so that no carbon would be able to condense if that interior were governed by chemical equilibrium.

We use an intentionally limited set of chemical species because our goal is to study the controversy over the correct carbon chemistry pathway to the ringed isomers. We limit the present study to C, O, CO, C<sub>2</sub>, C<sub>3</sub>, . . . C<sub>8</sub>, and C<sub>8</sub><sup>r</sup>, the ringed isomer of C<sub>8</sub>, to which we give a lifetime  $\tau_{\text{C}_8^{\text{r}}}^{\text{r}} = 10\text{ s}$  against thermal isomeric transition from linear C<sub>8</sub> to ringed C<sub>8</sub><sup>r</sup>. In a sense, the  $n = 8$  ring is a dummy standing for all rings, but is also reasonable in being the smallest ring that is widely expected (e.g., Takai et al. 1990). These ringed molecules are the seeds for carbon growth because their oxidation rates are much smaller than the oxidation rates of linear C<sub>n</sub>, whereas their C capture rates are fast. For the purpose of this study, we take ringed C<sub>8</sub><sup>r</sup> to be indestructible, simply integrating its rate of production. Our strategy is to compute the number C<sub>8</sub><sup>r</sup> remaining after expansion from two differing sources of C<sub>2</sub> initiating the linear C<sub>n</sub> chains. These two source reactions are

1.  $\text{C} + \text{C} \rightarrow \text{C}_2 + \gamma$  (Clayton et al. 1999) and
2.  $\text{CO} + \text{C} \rightarrow \text{C}_2 + \text{O}$  (Cherchneff & Dwek 2009, 2010).

We take our reaction rates from the rate tables in Cherchneff & Dwek (2009, 2010). The rate for the second reaction is indeed much greater than that of the first reaction above  $T = 3000\text{ K}$ , but it becomes increasingly the smaller of the two below  $T = 2500\text{ K}$ . We include the thermal inverse reaction of every reaction, which we calculate as in Equation (3) of Clayton et al. (2001). See Table 1 for sample thermal dissociation rates for CO molecules. We also include the dissociation of CO by Compton electrons in our network. CO is the only molecule for which electron dissociation can be the dominant destruction mechanism. For that rate we use  $\tau_e(\text{s}) = 10^5 \exp((t - 10^6\text{ s})/111\text{ days})$ , not fit to any specific model but with plausibility for SN 1987A. It increases to  $\tau_e = 10^6\text{ s}$  near eight months. Because of their helpful cataloging

of reaction rate tables, and in order to compare results without rate differences, we take the rates as given in the tables of Cherchneff & Dwek (2009, 2010). As an example, we take the rate for  $\text{C} + \text{C} \rightarrow \text{C}_2 + \gamma$  as the rate given by RA4 in Table 5 of Cherchneff & Dwek (2009).

Our computational reaction network is *libnucnet* (Meyer & Adams 2007; see also <http://sourceforge.net/projects/libnucnet/>) modified to follow the chemical rather than nuclear reactions. This network code has been thoroughly tested on a wide variety of reaction networks and problems. We scrupulously tested our network answers by manual calculations capable of exposing coding errors.

## 3. THE FUNCTION $n_{\text{CO}}(t)$

The interior core of C and O resulting from completed He burning in massive stars is a mix of C and O atoms having bulk  $\text{C}/\text{O} < 1$ . Post explosive cooling of such matter will attempt to associate C and O into CO molecules (Lepp et al. 1990). The reaction  $\text{C} + \text{O} \rightarrow \text{CO} + \gamma$  is one of the crucial reactions of chemical astrophysics. Its rate  $k_{\text{CO}}$  is intrinsically slow because quantum mechanics not only requires rearrangement of electronic shells but also simultaneous creation of a photon during the collision; nonetheless, the huge product  $n_{\text{C}}n_{\text{O}}$  in the He-exhausted core ensures steady growth for the CO abundance until it is reversed by radioactive dissociation.

Evidently, the abundance of CO within that zone during expansion attempts to balance these creation and destruction effects, doing so exactly at the time  $t = t_{\text{max}}$  of maximum  $n_{\text{CO}}$ . Clayton (2013) has discussed the shape of the function  $n_{\text{CO}}(t)$ . His Equation (1), which is valid at constant density, approximates the growth of  $n_{\text{CO}}$  by its leading terms:

$$\frac{dn_{\text{CO}}}{dt} = n_{\text{C}}n_{\text{O}}k_{\text{CO}} - \frac{n_{\text{CO}}}{\tau_{\text{CO}}} = 0 \quad (1)$$

at  $t = t_{\text{max}}$ . The maximum abundance reached by CO is in cgs units:

$$n_{\text{CO}}(t_{\text{max}}) = n_{\text{C}}n_{\text{O}}k_{\text{CO}}\tau_{\text{CO}}. \quad (2)$$

This amount is equal to that formed during its last mean lifetime  $\tau_{\text{CO}}$  against dissociation. Equation (2) is also highly accurate in circumstances where the time derivative in Equation (1) is but a small difference between much larger creation and destruction terms. Such balance is often set up as an abundance approaches its true maximum. If  $\tau_{\text{CO}}$  is taken to be  $\tau_\gamma$  as the dissociation of CO is dominated at  $T > 3500\text{ K}$  by thermal photons, one obtains the expression for the abundance  $n_{\text{CO}}^{\gamma\text{eq}}$  in thermal equilibrium:  $n_{\text{CO}}^{\gamma\text{eq}} = n_{\text{C}}n_{\text{O}}k_{\text{CO}}\tau_\gamma$ , and is also entered in Table 1.

Expressed instead in terms of number fractions  $Y_{\text{CO}} = n_{\text{CO}}/n$  and  $Y_{\text{C}} = n_{\text{C}}/n$  where  $n$  is the number density of all atoms,

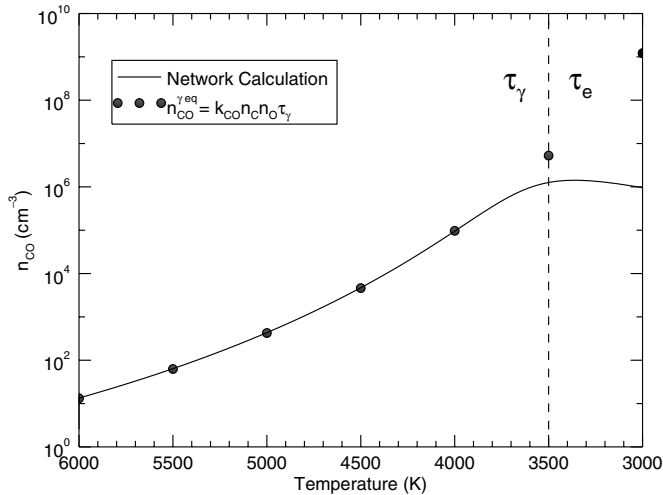


**Figure 1.** Comparison of the density of CO molecules calculated by the numerical network (curve) with the expectation  $n_{\text{CO}}^{\text{yeq}} = n_{\text{C}} n_{\text{O}} k_{\text{CO}} \tau_{\gamma}$  for an abundance  $n_{\text{CO}}$  in thermal equilibrium (dots) with photons. Above  $T = 4000$  K the CO abundance is seen to be in an accurate thermal equilibrium, but at lower temperature  $n_{\text{CO}}$  is increasingly smaller than that thermal equilibrium would require. Instead of thermal photons, the destruction of CO becomes increasingly dominated by Compton electrons for  $T < 3500$  K. One sees in Figure 1 that  $n_{\text{CO,max}}$  occurs near 3500 K, which occurs near  $10^7$  s (see Table 1).

Equation (1) transforms to

$$\frac{dY_{\text{CO}}}{dt} = Y_{\text{C}} Y_{\text{O}} n k_{\text{CO}} - \frac{Y_{\text{CO}}}{\tau_{\text{CO}}}, \quad (3)$$

which is the form integrated by our network of coupled reactions. The number density  $n$  is needed for the rate  $n(\text{cm}^{-3})k_{\text{CO}}(\text{cm}^3 \text{s}^{-1})$ . In our numerical example, we take  $n_{\text{O}} = 10^{10} \text{ cm}^{-3}$  and  $n_{\text{C}} = 10^9 \text{ cm}^{-3}$  at  $t_{6000 \text{ K}}$  as starting conditions for the chemical network. Subsequent values are  $n = 1.1 \times 10^{10} \text{ cm}^{-3} (t_{6000 \text{ K}}/t)^3$ , where the expansion factor reduces the initial number density appropriately. The expansion factors are also given in Table 1. Then, Equation (2) reads

$$Y_{\text{CO}}(t_{\text{max}}) = Y_{\text{C}} Y_{\text{O}} n k_{\text{CO}} \tau_{\text{CO}}, \quad (4)$$

which is valid during expansions.

The lifetime of CO against dissociation is a composite of two physical reactions. Letting  $\tau_{\gamma}$  be the photodissociation lifetime owing to thermal photons and  $\tau_e$  be the dissociation lifetime owing to fast Compton electrons, we have

$$\frac{1}{\tau_{\text{CO}}} = \frac{1}{\tau_{\gamma}} + \frac{1}{\tau_e}. \quad (5)$$

The partial lifetime that dominates the dissociation depends on the temperature. The radioactive lifetime  $\tau_e$  is taken to be  $\tau_e(\text{s}) = 10^5 \exp((t - 10^6 \text{ s})/111 \text{ days})$ , but the thermal photodissociation lifetime  $\tau_{\gamma}$  depends strongly on temperature owing to the large binding energy of the CO molecule. Table 1 displays a short list of  $\tau_{\gamma}$  at key temperatures as well as several related quantities.

One sees from Table 1 that  $\tau_{\gamma}$  dominates Equation (5) for  $T > 3500$  K, whereas Compton electron dissociation  $\tau_e$  dominates below 3500 K. We start computation of our chemical network at  $T = 6000$  K, so  $n_{\text{CO}}(t)$  will initially be small and will grow as the temperature declines owing to the increase in  $\tau_{\gamma}$  with falling temperature. After  $t = t_{\text{max}}$ , the abundance of CO declines owing to the destruction rate  $1/\tau_e$  exceeding the

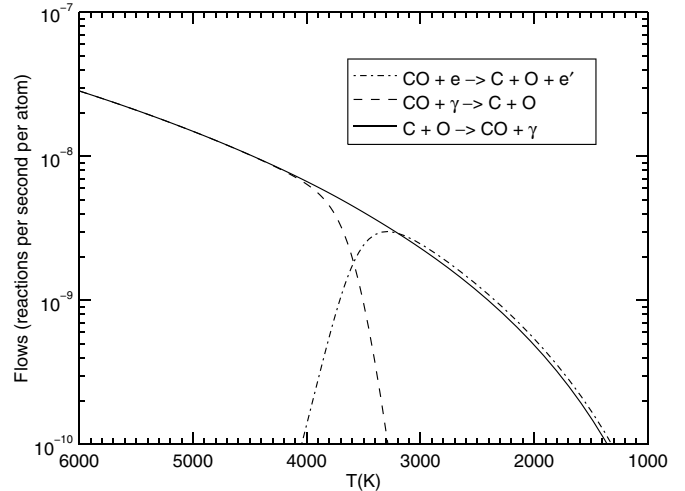


**Figure 2.** Flows into and out of CO illustrate the near steady state between creation and destruction and the transition region near 3500 K between the two modes of destruction of CO. The destruction flow  $n_{\text{CO}} n_{\text{C}} k_{\text{CO}+\text{C}}$  is only  $3.27 \times 10^{-16} \text{ atom}^{-1} \text{ s}^{-1}$ , too small to be visible here.

creation rate in Equation (1) while the gas cools to temperatures at which carbon chains can grow and isomerize to rings (Clayton et al. 1999). Such rings are taken to be the nucleations upon which graphite grows.

Figure 1 compares our network calculation of the abundance of CO molecules with the expectation of Equation (2) with  $\tau_{\text{CO}} = \tau_{\gamma}$  dominating the destruction of CO. The solid points display the equilibrium product  $n_{\text{CO}}^{\text{yeq}}$  calculated from the factors shown in Table 1 and from the number densities  $n_{\text{C}}$  and  $n_{\text{O}}$  after their initial values at  $T = 6000$  K have been reduced by the expansion factor  $(t/t_{6000 \text{ K}})^{-3}$ . Tight agreement for  $T > 4000$  K is immediately evident, demonstrating that for  $T > 4000$  K the abundance of CO is almost exactly in thermal equilibrium. Equation (2) validly describes the black dots in Figure 1 because creation and destruction terms are very nearly balanced while  $T > 4000$  K. Below 3500 K, the abundance of CO becomes much smaller than the expectation  $n_{\text{CO}}^{\text{yeq}}$  of thermal equilibrium because the dissociation of CO comes to be dominated by Compton electrons. The dashed vertical line at  $T = 3500$  K marks the approximate boundary between these two mechanisms for CO dissociation. Note carefully in Figure 1 that  $n_{\text{CO}}$  grows slowly as  $T$  falls, not reaching its final maximum until expansion has cooled to  $T = 3500$  K. Although it is obvious that equilibrium CO increases as  $T$  falls, assuming that to occur begs the question of achieving equilibrium. Our kinetic results demonstrate that CO does quickly achieve its equilibrium abundance above  $T = 4000$  K, and Equation (3) shows that equilibrium increases as  $\tau_{\gamma}$  increases. At its final maximum  $n_{\text{CO}} = 1.5 \times 10^6 \text{ cm}^{-3}$ , corresponding to  $Y_{\text{CO}} = 0.7 \times 10^{-3}$ . The slow growth of  $n_{\text{CO}}$  shown in Figure 1 differs markedly from the results of Cherchneff & Dwek (2009). Their results (e.g., Figure 11) show  $n_{\text{CO}}$  climbing quickly near 6000 K to a large maximum number fraction near 0.1. This maximum would almost exhaust free carbon. Our results in Figure 1 so differ from theirs that the difference must be resolved. Clayton (2013) has analyzed the expectation of the growth of  $n_{\text{CO}}$  to a single maximum before declining, and our results are in line with that expectation.

These features are further detailed in Figure 2, which shows the reaction currents (reactions per second per atom) into and out of CO. There exists a near steady state in that the production

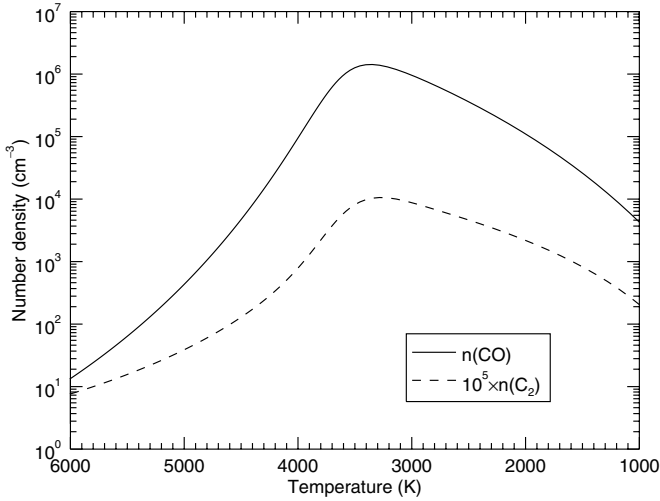


**Figure 3.** Number densities of CO and of C<sub>2</sub> as functions of temperature. The maximum density of C<sub>2</sub> is 0.1 cm<sup>-3</sup>. Both the abundances grow much more slowly than in the calculation by Cherchneff & Dwek (2009).

of CO is almost balanced by the two flows destroying CO. The destruction flow  $Y_{\text{CO}}/\tau_\gamma$  almost balances the association flow above 4000 K except for a tiny excess leading to the slow growth of  $n_{\text{CO}}$  evident in Figure 1. In this temperature range the production by  $\text{C} + \text{O} \rightarrow \text{CO} + \gamma$  is in equilibrium with the thermal radiation field, as Figure 1 implies. The decline of the flow creating CO occurs owing to expansion. The destruction flow  $n_{\text{CO}}/\tau_e$  almost balances the creation flow below 3500 K. The transition between destruction modes occurs near 3500 K. It is no coincidence that the maximum of  $n_{\text{CO}}$  occurs when Compton electrons begin to dominate CO dissociation, because  $n_{\text{CO}}$  would continue growing as long as thermal photons dominate CO dissociation. Figure 2 also shows the destructive flow by inelastic electrons to slightly exceed the production flow for  $T < 3500$  K. This modest difference causes CO to decline following its maximum.

#### 4. ABUNDANCES OF C<sub>n</sub>

Figure 3 displays the number density  $n_{\text{C}_2}$  along with that of  $n_{\text{CO}}$ . Our examination of flows into C<sub>2</sub> shows that the reaction  $\text{CO} + \text{C} \rightarrow \text{C}_2 + \text{O}$  competes with the reaction  $\text{C} + \text{C} \rightarrow \text{C}_2 + \gamma$  only in the range  $3400 \text{ K} < T < 3900 \text{ K}$ , but falls steeply for greater or lesser temperature. At higher  $T$  the abundance of CO is too small to create C<sub>2</sub> in this way, and at smaller  $T$  the cross section for  $\text{CO} + \text{C} \rightarrow \text{C}_2 + \text{O}$  declines too precipitously. Cherchneff & Dwek (2009) missed that because their calculated abundance of CO was much too large. At its maximum,  $n_{\text{C}_2} = 0.1 \text{ cm}^{-3}$  is only about  $10^{-7}$  of  $n_{\text{CO}}$ . The reason why C<sub>2</sub> is so rare is that its dissociation rate by thermal photons is much faster than that for CO because the binding energy of C<sub>2</sub> is so much less than that for CO. The smaller value of  $\tau_\gamma$  causes the steady state with thermal radiation for C<sub>2</sub>, as in Equation (3), to be much smaller than that for CO, so  $n_{\text{C}_2}$  grows much more slowly than  $n_{\text{CO}}$ . The Compton electron lifetime  $\tau_e$  never plays a role for C<sub>2</sub>, but the lifetime against oxidation becomes faster than  $\tau_\gamma$  when  $T$  falls below 3500 K. This transition establishes the maximum in Figure 3. The  $n_{\text{C}_2}$  maximum differs greatly from the results in Cherchneff & Dwek (2009), where Figure 11 shows the maximum atom fraction of  $n_{\text{C}_2}$  to be near  $10^{-5}$ , equal to about  $10^5 \text{ cm}^{-3}$ , almost 1% of their  $n_{\text{CO}}$  at that time. Their maximum

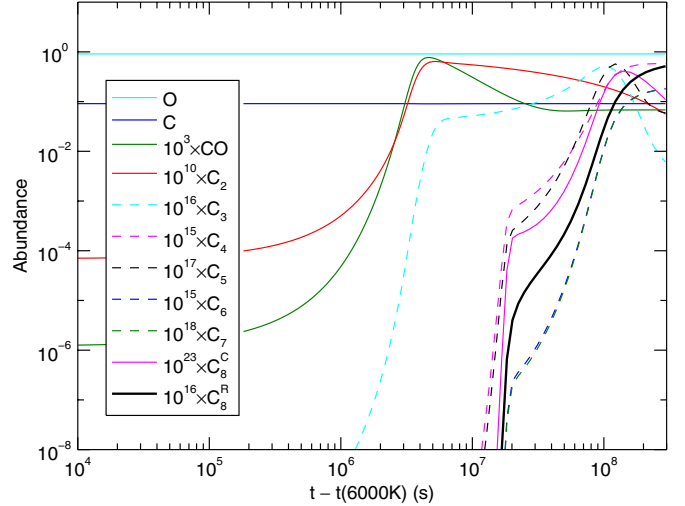


**Figure 4.** Abundance (number per atom) of linear chains C<sub>n</sub> and ringed isomer C<sub>8</sub><sup>r</sup>. We have scaled each Y<sub>n</sub> by the factor stated in the box.

for C<sub>2</sub> occurs near 7000 K, far too hot for C<sub>2</sub> to be abundant in the face of rapid photodissociation. The huge differences between these two computations require an explanation. We find it likely that Cherchneff & Dwek (2009) inadvertently omitted photodissociation by thermal photons from their destruction rates.

Figure 4 shows the abundances  $Y_i$  of each species in our small network as a function of time  $t - t_{6000 \text{ K}}$  after  $T = 6000$  K. From Table 1, the start time is  $t_{6000 \text{ K}} = 5.47 \times 10^6$  s. To display each  $Y_i$  on a figure with reasonable ordinate resolution, we have scaled each  $Y_n$  by the factor stated in the box. Many features are noteworthy: (1)  $Y_{\text{C}}$  and  $Y_{\text{O}}$  are constant because their small depletion is negligible on the scale shown; (2) maxima of  $Y_{\text{CO}}$  and  $Y_2$  occur at almost exactly the same time  $t - t_{6000 \text{ K}} = 4 \times 10^6$  s, as was also seen in Figure 3; (3) C<sub>3</sub> has very small abundance, about  $10^{-7}$  of  $Y_2$ , although much later  $Y_3$  slowly grows modestly relative to much more abundant C<sub>2</sub>; (4) the rise shapes of  $Y_4$  through  $Y_8$  are very similar because they are linked by a near steady state; (5) the ringed carbon abundance  $Y_8^r$  has similar abundance shape versus time, but note that it is actually much more abundant than linear C<sub>7-8</sub> and because it accumulates from isomeric transitions of C<sub>8</sub> and unlike C<sub>n</sub> does not suffer from fast oxidation (Clayton et al. 1999). Each of these features is understandable in terms of the flows into and out of each species.

One sees from Figure 4 that the  $\text{CO} + \text{C} \rightarrow \text{C}_2 + \text{O}$  reaction plays no role in C<sub>8</sub><sup>r</sup> production from the fact that C<sub>8</sub><sup>r</sup> rises only for  $t - t_{6000 \text{ K}} > 1.5 \times 10^7$  s, corresponding to  $T < 2000$  K, despite C<sub>2</sub> and C<sub>3</sub> rising at much earlier times. Whatever C<sub>2</sub> is made earlier plays no role in C<sub>8</sub><sup>r</sup> production because the ejection of C atoms from C<sub>n</sub> at higher  $T$  prevents the flow to C<sub>8</sub>. Only at  $T < 2000$  K do those photodissociation reactions become so slow that C<sub>8</sub> can grow, which it does from the C<sub>2</sub> recently formed by the  $\text{C} + \text{C} \rightarrow \text{C}_2 + \gamma$  reaction near 2000 K. Figure 4 also shows that  $Y_8^r$  quickly grows to  $10^{-16}$ . Since available C is  $Y_{\text{C}} = 0.1$ , the ratio gives  $10^{15} \text{ C ring}^{-1}$ . This is enough to grow very large graphite.

Figure 5 shows the shape of C<sub>n</sub> versus  $n$  for C<sub>3</sub> to C<sub>8</sub> at two different temperatures near 2000 K. As the temperature declines, the curve flattens because photoejection from C<sub>n</sub> by thermal photons (or vibrations) weakens. These abundance ratios are almost in a steady state, but this steady state changes slightly as  $T$  falls. These patterns show almost equal values for  $Y_3$  because

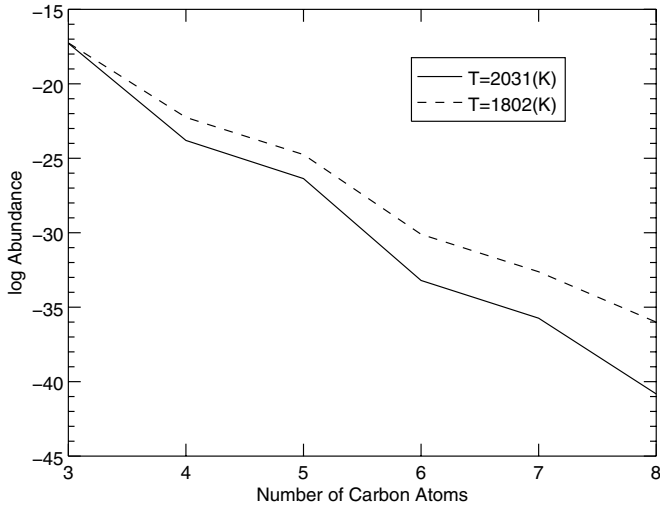


**Figure 5.** Shape of  $\log 10(Y_n)$  vs.  $n$  for  $C_3$  to  $C_8$  at two different temperatures near 2000 K. These shapes can be understood by the relative magnitudes of flows into and out of  $C_n$ .

that curve is relatively flat with time near  $t - t_{6000\text{ K}} = 10^7\text{ s}$  (Figure 4). Table 2 lists our computed reaction flows both in and out of  $C_6$  at  $T = 2031\text{ K}$  and  $T = 1802\text{ K}$ . The reactions are specified there in the compact notation target(in,out)residual. We tabulate the flow magnitudes for  $C_6$  to aid readers checking our numerical results. Figure 5 and Table 2 should be studied together. Note that the abundances of  $C_8$  are very small:  $Y_8 = 10^{-36}$  at  $T = 1802\text{ K}$ . The isomeric transition from linear to ringed  $C_8$ , for which we estimate a lifetime  $\tau = 10\text{ s}$ , provides the nucleations for graphite growth.

We call attention to several conclusions to be drawn from Table 2. First, the strongest flows by a wide margin involving  $C_6$  are  $C_5 + C \rightarrow C_6$ , which is very fast ( $k = 3 \times 10^{-10}\text{ cm}^3\text{ s}^{-1}$ ) because vibrational excitation of  $C_6$  obviates the need for creating a photon (Clayton et al. 1999), and its inverse reaction which ejects a C atom. Furthermore, those two flows are equal to each other to three significant figures, illustrating the near steady state of the abundance pattern. Second, thermal dissociation of  $C_6$  is very much faster than its oxidation, showing the small effect of oxidation on the abundance pattern. The destroying flows from  $C_6$  to  $C_5$  stand in the approximate ratio  $C_6(\gamma, C)/C_6(O, CO) = 5 \times 10^5$  at  $T = 2031\text{ K}$  and  $2 \times 10^4$  at  $T = 1802\text{ K}$ . Dissociation by thermally excited vibrations dominates oxidation. What we label  $(\gamma, C)$  here is actually radiationless. Note that the oxidation of  $C_n$  molecules is not faster than C-ejection reactions. This unusual situation occurs because the C-capture reactions proceed by exciting vibrations of the  $C_6$  molecule. This residual vibrational energy makes capture reactions fast rather than slow, but also makes the inverse C-ejection reactions caused by thermally excited vibrations to be much faster. Detailed balance gets the ratio right. The smaller value for that ratio at  $T = 1802\text{ K}$  occurs because oxidation maintains its effectiveness as  $T$  drops but thermal disruption does not, being much more temperature sensitive. For this reason, the abundance pattern is flatter and  $C_6$  is approximately 3000 times more abundant at  $T = 1802\text{ K}$  than at  $T = 2031\text{ K}$ . It is for this reason that destruction flows in Table 2 for  $C_6$  are larger at the smaller temperature. The steady state shifts to new ratios as  $T$  falls. Thirdly, calculation of the rates will be illustrated for the sake of clarity by the flow  $C_6 + O \rightarrow CO + C_5$ . From Figure 5, one sees that at  $T = 2031\text{ K}$  the abundance  $Y_6 = 10^{-33.3}$ . The value of  $Y_O = 10^{10}\text{ cm}^{-3}/1.1 \times 10^{10}\text{ cm}^{-3} = 0.909$ , so

**Table 2**  
Reaction Flows Involving  $C_6$  at Two Temperatures

Reaction	Flow ( $\text{atom}^{-1}\text{ s}^{-1}$ )	
	$T = 2031\text{ K}$	$T = 1802\text{ K}$
$C_5(C, \gamma)C_6$	$1.67 \times 10^{-29}$	$4.79 \times 10^{-28}$
$C_6(\gamma, C)C_5$	$1.67 \times 10^{-29}$	$4.79 \times 10^{-28}$
$C_6(C, \gamma)C_7$	$2.41 \times 10^{-39}$	$2.12 \times 10^{-32}$
$C_7(\gamma, C)C_6$	$1.26 \times 10^{-40}$	$7.27 \times 10^{-40}$
$C_6(O, CO)C_5$	$3.61 \times 10^{-31}$	$2.90 \times 10^{-32}$

the flow per atom per second (e.g., Equation (3)) is  $dY/dt = Y_6 Y_O n(2031\text{ K})k(C_6 + O)$ . The expansion from  $T = 6000\text{ K}$  to  $T = 2031\text{ K}$  has diluted the total number density  $n$  to  $1.1 \times 10^{10}\text{ cm}^{-3} (2031\text{ K}/6000\text{ K})^3 = 4.27 \times 10^8\text{ cm}^{-3}$ . The fast oxidation reaction rate factor is  $k(C_6 + O) = 3 \times 10^{-10}\text{ cm}^3\text{ s}^{-1}$ . Gathering factors yields approximately  $4 \times 10^{-35}$  per atom per second in good approximation to the Table 2 flow entry  $3.61 \times 10^{-35}$  per atom per second.

Our calculations have clearly shown that producing  $C_2$  molecules near 5000 K via the  $CO + C$  reaction (Cherchneff & Dwek 2009) is not a viable prospect for the condensation of carbon dust via linear carbon chains. The abundance of CO is far too small for it to seed high- $T$   $C_2$  production. The abundance of  $C_8$  rings grows much later (Figure 4) near 2000 K, as found by Clayton et al. (1999, 2001). These rings grew from  $C_2$  created by simple carbon association,  $C + C \rightarrow C_2 + \gamma$ . Furthermore, the abundance of  $C_2$  is very small near 5000 K (Figure 3), primarily because its thermal dissociation rate is much too fast for it to have significant abundance at that high  $T$ . Whatever little  $C_2$  is made at 5000 K is immediately dissociated by thermal photons. Therefore its small steady-state abundance is inadequate for building abundances of  $C_3$  and beyond.

## 5. CONTRAST WITH CHERCHNEFF & DWEK (2009, 2010)

The large numerical differences between the results of Clayton et al. (1999, 2001) and those of Cherchneff & Dwek (2009, 2010) seem to be characterized by the following differences.

1. Instead of growing large CO abundance near  $Y_{CO} = 0.1$  at  $T = 5500\text{ K}$  as in Figure 11 of Cherchneff & Dwek (2009), we find that  $Y_{CO}$  builds to a maximum of only  $10^{-3}$ , which it achieves only slowly (Figure 3), reaching that maximum only at  $T = 3500\text{ K}$  rather than 5500 K.
2. We find a maximum number density  $n_{C_2} = 0.1\text{ cm}^{-3}$ , which is only about  $10^{-7}$  of  $n_{CO}$ . We find  $C_2$  to be rare at high temperature because its dissociation rate by thermal photons is very much faster than for CO owing to the smaller binding energy (6.3 eV) of  $C_2$ . This  $n_{C_2}$  maximum differs greatly from the results in Cherchneff & Dwek (2009), where their Figure 11 shows the maximum atom fraction of  $n_{C_2}$  to be near  $10^{-5}$ , equal to about  $10^5\text{ cm}^{-3}$ , almost 1% of  $n_{CO}$  at that time. Our  $C_2/CO$  abundance ratio is, in other words, only  $10^{-5}$  of the same ratio calculated by Cherchneff & Dwek (2009).

These big differences can be understood if Cherchneff & Dwek (2009) had inadvertently omitted the thermal dissociation rates of small carbon molecules. Considering this to be the cause for the discrepancy, we tested that hypothesis by performing our own trial calculation involving only C, O, CO,  $C_2$ , and  $C_3$ , as

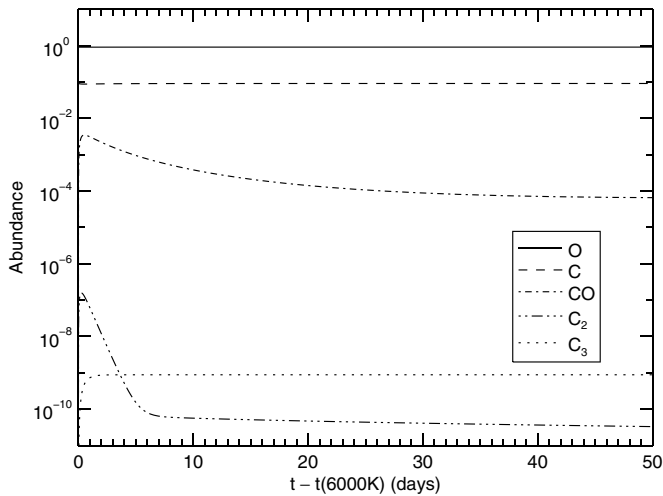


**Figure 6.** Abundances for network containing only C, O, CO, C<sub>2</sub>, and C<sub>3</sub> when photodissociation of molecules is omitted. The rapid rise of  $Y_{\text{CO}}$  to  $10^{-2}$  near 5500 K and the ratio  $Y_{\text{CO}}/Y_2$  near  $10^4$  are similar to Figure 11 of Cherchneff & Dwek (2009).

done by them, and omitted the  $\tau_\gamma$  destruction terms and the oxidation of C<sub>3</sub>. The result is displayed in Figure 6. The rapid rise of  $Y_{\text{CO}}$  to about  $10^{-2}$  at high temperature is very similar to Figure 11 of Cherchneff & Dwek (2009). Also similar is  $Y_2$ , which grows quickly (Figure 6) to  $2 \times 10^{-4}$  of  $Y_{\text{CO}}$ , whereas our Figure 3 shows the true value of  $Y_{\text{CO}}$  to be only  $10^{-8}$  at  $T = 5500$  K and, considerably later,  $Y_2/Y_{\text{CO}} = 10^{-7}$  at their maxima.

With photodissociation turned off, the destruction of C<sub>2</sub> occurs primarily by oxidation,  $\text{C}_2 + \text{O} \rightarrow \text{CO} + \text{C}$ , whereas the production of C<sub>2</sub> is by  $\text{CO} + \text{C} \rightarrow \text{C}_2 + \text{O}$ , the reaction we study in this work. These reactions strive to balance, which if achieved would establish a steady-state ratio  $Y_{\text{CO}}/Y_2 = 3.5 \times 10^4$ . Figure 6 and their Figure 11 do approximately show this value, but  $Y_2$  declines faster than  $Y_{\text{CO}}$  because of declining production of C<sub>2</sub> as  $T$  declines.

We could not expect detailed agreement with Cherchneff & Dwek (2009) even if our hypothesis for the cause of the discrep-

ancy is correct. Our calculation used  $\text{O}/\text{C} = 10$  whereas theirs used  $\text{O}/\text{C} = 3$  for the zone of their SNI model. The temperature profiles also differ; we use  $T = 3800 \text{ K}/(t/100 \text{ days})$  and they used  $T = 18,500 \text{ K}/(t/100 \text{ days})^{1.8}$ . We believe that their  $T$  is too hot owing to omission of CO cooling (Liu & Dalgarno 1996; Figure 5), which we tried to accommodate roughly by the choice  $T = 3800 \text{ K}$  at  $t = 100$  days, which is about 50% of the temperatures published within models that do omit CO cooling. Owing to the factor  $t^{-1.8}$ , their  $T$  falls through a specified temperature drop (say 5000 K to 3000 K) more quickly than does our parameterization. Nonetheless, any  $T$  profile declines through 5000 K and reaches 3000 K somewhat later, so basically similar abundance results are expected.

Such detailed differences are small in comparison with the inclusion of thermal photodissociation. The similarity of our Figure 6 to Figure 11 of Cherchneff & Dwek (2009) and the huge differences of these figures from those of our network are considered to resolve the discrepancy.

T.Y. gratefully acknowledges the support of the NASA Earth and Space Science Fellowship. This work was also supported by NASA grant NNX10AH78G.

## REFERENCES

- Cherchneff, I., & Dwek, E. 2009, *ApJ*, 703, 642  
 Cherchneff, I., & Dwek, E. 2010, *ApJ*, 713, 1  
 Clayton, D. D. 2011, *NewAR*, 55, 155  
 Clayton, D. D. 2013, *ApJ*, 762, 5  
 Clayton, D. D., Deneault, E. A.-N., & Meyer, B. S. 2001, *ApJ*, 562, 480  
 Clayton, D. D., Liu, W., & Dalgarno, A. 1999, *Sci*, 283, 1290  
 Clayton, D. D., & The, L.-S. 1991, *ApJ*, 375, 221  
 Deneault, E. A.-N., Clayton, D. D., & Heger, A. 2003, *ApJ*, 594, 312  
 Deneault, E. A.-N., Clayton, D. D., & Meyer, B. S. 2006, *ApJ*, 638, 234  
 Klots, C. E. 1968, in *Fundamental Processes in Radiation Chemistry*, ed. P. Ausloos (New York: Interscience), 40  
 Lepp, S., Dalgarno, A., & McCray, R. 1990, *ApJ*, 358, 262  
 Liu, W., & Dalgarno, A. 1996, *ApJ*, 471, 480  
 Liu, W., & Victor, G. A. 1994, *ApJ*, 435, 909  
 Meyer, B. S., & Adams, D. C. 2007, in *70th Annual Meteoritical Society Meeting, 2007 August 13–17, Tucson, Arizona, Meteoritics and Planetary Science Supplement*, Vol. 42, 5215  
 Takai, T., Lee, C., Halicioglu, T., & Tiller, W. A. 1990, *JPhCh*, 94, 4480